

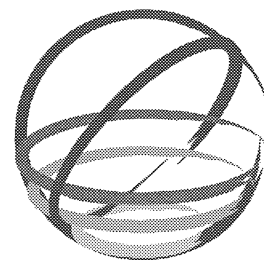
# A Curves Approximated Multiple-Spring Model Seismic Response Simulation for Square-Section Steel Bridge Piers

**J. Dang & A. Igarashi**

*Kyoto University, Kyoto, Japan*

**T. Aoki**

*Aichi Institute of Technology, Aichi Ken, Japan*



**15 WCEE**  
LISBOA 2012

## **SUMMARY: (10 pt)**

In this study, a seismic response simulation method based on the multiple-spring (MS) model and constitutive rules using curve approximation is proposed to predict nonlinear seismic response of steel bridge piers with rectangular cross-sections excited by bi-directional ground motions. A series of approximated curves and hysteretic rules are adopted to the nonlinear equivalent stress-strain relationship of spring elements distributed on the base cross-section of a thin-walled steel column. In this process, the strain of each spring can be calculated from the column's bi-directional displacements and the geometric coordinates, while the bi-directional horizontal restoring force can be obtained by the spring forces calculated by the springs' stress and tributary areas. To verify the accuracy of the proposed model, results of 6 uni-directional pseudodynamic tests and 3 bi-directional pseudodynamic tests are compared with numerical simulation results. The validity of the proposed method is demonstrated by good accuracy in restoring force and response displacement between the test results and numerical simulations.

*Keywords: bi-directional seismic response, steel bridge pier, multiple-spring model, constitutive rule*

## **1. INTRODUCTION**

Elevated steel bridge piers are widely constructed in urban area of major city of Japan. After experiencing severe damage and collapse of steel bridge piers during the 1995 Hanshin-Awaji Earthquake, the design codes for steel structures were immediately revised and the performance based design concept was introduced to practical design. The present Specification for Highway Bridges of Japan (Japan Road Association, 2002) suggests verifying the seismic response demand by credible and properly configured time domain nonlinear simulation methods.

The steel columns are generally considered and analysed as uni-axial flexure cantilever beams in current seismic design by conducting nonlinear response simulation in two orthogonal directions separately or independently, in accordance with an idealized situation that the earthquake attacks the structure only in one major direction. However, the actual seismic load acts on structures in three dimensions. For bridge piers, the interaction between the structural responses in the two directions should be taken into account in designing for severe seismic motions in order to assure the safety and performance of steel piers.

Bi-directional quasi-static and hybrid tests have been conducted by Nagata K. (2004), Watanabe E. (2005), Goto Y. (2007, 2009), Aoki T. (2007) and Dang J. (2010) etc., to investigate the difference in restoring force and response displacement between uni- and bi-directionally loaded steel bridge columns. According to these tests, the difference between tests with and without orthogonal directional loading could be about 4%~36% in the restoring force and 20%~30% in the response displacement. These strength and response differences of uni- and bi-directionally loaded bridge piers are significant, and are difficult to be predicted by the conventional over-simplification in-plane uni-directional simulation methods.

Therefore, for reliable evaluation of the seismic performance of steel columns, an effective and efficient numerical method accounting for both the hysteretic restoring character of steel piers and the interactive effects under bi-directional flexure loading is desirable, in order to perform not only practical design preferably based on accurate and less time-consuming simulation, but also numerical study to determine a compromised reduction factor on a statistical basis.

The multiple-spring (MS) model is a convenient numerical method to simulate the bi-directional seismic response of both RC (Lai, 1984) and steel (Jiang, 2001, 2002) structures, and those with isolation devices (Ishii, 2010). Although seismic response simulation methods for unstiffened circular section steel columns by the MS model have been discussed in the recent decade by comparing with FEM analysis, the modelling procedure for the stiffened thin-walled square-section column, which is the mostly constructed type of steel columns for both bridge piers and building columns, and experimental verification, especially those by response tests, are essential to refine this method to the next practical stage.

In this study, a practical modelling procedure for the MS model analysis of hollow box steel columns and a series of constitutive laws using curve approximation for the model springs are discussed to evaluate the bi-directional hysteretic flexure behavior and bi-directional seismic response performance. Furthermore, bi-directional pseudodynamic test results are used to clarify the validity of this method.

## 2. OUTLINE OF MS MODEL FOR HOLLOW BOX COLUMN

In the MS model for rectangular thin-walled steel piers of cantilever type, the lateral deformation of a column is assumed to be expressed by the concentrated springs located on the base section under a non-deformable rigid bar, as shown in Fig. 2.1. The mass and weight of the superstructure is represented by a point mass on the top of the rigid bar.

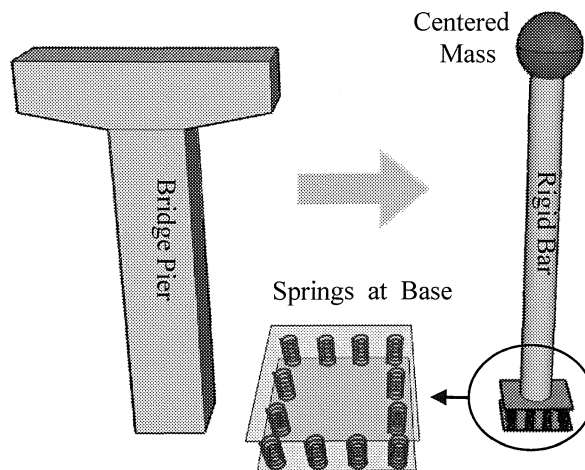


Figure 2.1. Multiple-Spring Model

The geometric properties, location and tributary area etc., of each spring are obviously important in representing the deformation behaviour of the column by the base section springs. These geometric properties can be usually determined by dividing the cross section to some small elements, as shown in Fig. 2.2. The stiffened cross section, such as that shown in Fig. 2.2(a), can be simplified as a mechanically equivalent non-stiffened section with the identical second moment of areas  $A$ , width  $b$  and a different equivalent plate thickness  $t_e$  from the original stiffened section, as shown in Fig. 2.2(b). A quarter of this section, shown in Fig. 2.2(c), can be divided into small elements of number  $n$ . Therefore, the whole cross section can be equivalently seen as  $4n$  springs which have their area  $A_i$  and coordinates  $(x_i, y_i)$  ( $i= 1, 2, \dots$ ) coinciding with the area and the centroid of the elements

dividing the equivalent unstiffened section. Here, the subscript  $i$  present a spring number.

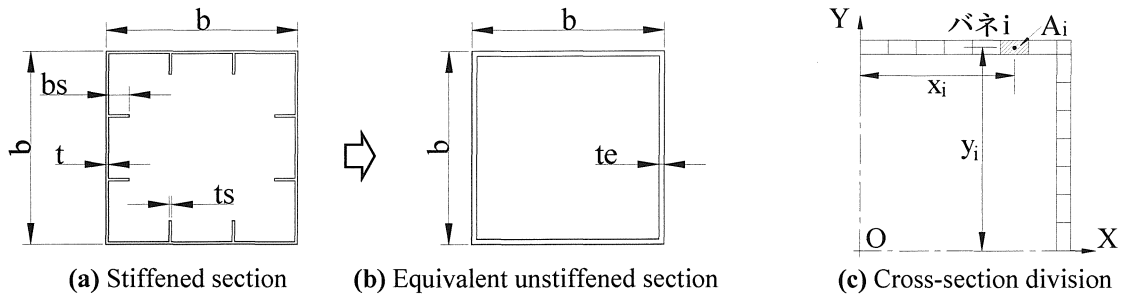


Figure 2.2. Cross-section division for stiffened and unstiffened column

According to the Euler-Bernoulli hypotheses (the plan section assumption), the strain of the  $i^{\text{th}}$  spring  $\varepsilon_i$ , can be calculated from the bi-directional displacement  $(\delta_x, \delta_y)$  by following equation.

$$\varepsilon_i = (\delta_x x_i + \delta_y y_i)/hl \quad (2.1)$$

where,  $h$  is the height of the column and  $l(=1)$  is the representative height of the springs.

It can be considered that the strain of two springs at symmetric positions of a column under any bi-directional flexure, e.g. spring  $i$  and spring  $j$  in Fig. 2.3(a), should agree with each other in the value but opposite in sign ( $\varepsilon_j = -\varepsilon_i$ ), as shown in Fig. 2.3(b). To simplify the approach, the stress of the two springs is considered to be in symmetry ( $\sigma_j = -\sigma_i$ ), although there are considerable differences in the behaviours of steel members in tension and under compression, such as the effect of local buckling and strain hardening etc. Therefore, the constitutive relation should account for the inelastic behaviours of the combined two steel plates, and the stress  $\sigma$  is only an equivalent value to represent the bending moment by the tension and pressure spring forces. Hence the horizontal forces  $(H_x, H_y)$  in the two orthogonal directions can be calculated by integrating the stress of springs of only a half section using the following equation:

$$H_x = (2 \sum_{i=1}^{2n} \sigma_i A_i x_i - P \delta_x)/h \quad (2.2)$$

$$H_y = (2 \sum_{i=1}^{2n} \sigma_i A_i y_i - P \delta_y)/h \quad (2.3)$$

where  $P$  presents the constant vertical force.

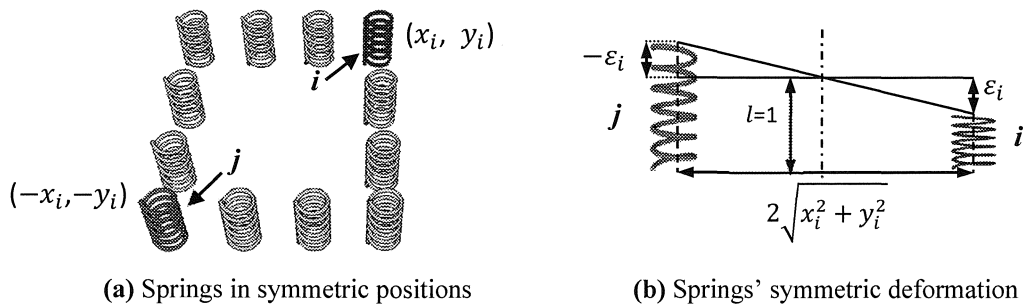


Figure 2.3. Equivalent strain

### 3. NONLINEAR CONSTITUTIVE LAWS OF SPRINGS

The aforementioned assumption of symmetry ( $\varepsilon_j = -\varepsilon_i$ ;  $\sigma_j = -\sigma_i$ ) is considered in the determination of the constitutive laws for the MS model of steel piers similar to that of SDOF hysteretic model. Accordingly, the method presented in this study can also be interpreted as a procedure such that the two dimensional nonlinear behaviour of steel columns is divided into  $2n$  lateral directions defined by

those coordinates of springs  $(x_i, y_i)$  and applying constitutive laws similar to that of hysteretic restoring force-displacement relationship followed by a process of gathering these stress to integrate the bi-directional horizontal force of the column subjected to inelastic deformation. Several hysteretic models for steel bridge columns have been proposed, and one of the most effective models referred to as the approximated curve model is employed as the constitutive law for the springs in this study.

### 3.1. Elastic modulus

Considering the stiffness softening due to deterioration after the peak load, the elastic modulus  $E$  of the springs'  $\sigma - \varepsilon$  relationship should be decreased with the cumulative deterioration as will be discussed later. The initial value of elastic modulus  $E_0$  can be found from the yield stress  $\sigma_0$  and the yield strain  $\varepsilon_0$ .

$$E_0 = \sigma_0 / \varepsilon_0 \quad (3.1)$$

The yield strain  $\varepsilon_0$  is defined as the largest strain of the springs when the displacement of the column is uni-directionally loaded to the yield displacement  $\delta_0$ . It follows that  $\varepsilon_0$  can be calculated from  $\delta_0$  by the following equation.

$$\varepsilon_0 = \delta_0(b - t_e) / 2hl \quad (3.2)$$

The yield stress corresponding to the horizontal yield force, the vertical loading and the yield displacement  $\delta_0$  can be found by the following equations.

$$\sigma_0 = M_0 / Z_e \quad (3.3)$$

$$M_0 = H_0 h + \delta_0 P \quad (3.4)$$

$$Z_e = 2 \sum_{i=1}^{2n} x_i^2 A_i / (b/2 - t_e/2) \quad (3.5)$$

where  $M_0$  represents the yield moment of the cross-section and  $Z_e$  represents the section modulus of the equivalent section consisting of the springs.

### 3.2. Envelope curves

The envelope curve of the nonlinear  $\sigma - \varepsilon$  relationship shown in Fig. 3.1 contains a basic curve part before peak point  $(\varepsilon_m, \sigma_m)$  and a deterioration curve part between the peak point and the ultimate boundary point  $(\varepsilon_u, \sigma_u)$ . The basic curve is approximated by a cubic curve to express the slop of  $\sigma - \varepsilon$  relationship changing from  $E$  to 0 and the stress changing from 0 to  $\sigma_m$  as the strain varies from 0 to  $\varepsilon_m$ . The stress of a spring in the basic curve part can be calculated from its strain  $\varepsilon$  by the following approximated cubic curve equation.

$$\sigma = E\varepsilon + \varepsilon^2(3\sigma_m - 2E\varepsilon_m) / \varepsilon_m^2 + \varepsilon^3(E\varepsilon_m - 2\sigma_m) / \varepsilon_m^3 \quad (3.6)$$

The deterioration curve expresses the decrease of bearing capacity after the peak point. This curve can be expressed by the following equation.

$$\sigma = \sigma_m + 2(\varepsilon - \varepsilon_m)(\sigma_u - \sigma_m) / (\varepsilon_u - \varepsilon_m) - (\varepsilon - \varepsilon_m)^2(\sigma_u - \sigma_m) / (\varepsilon_u - \varepsilon_m)^2 \quad (3.7)$$

### 3.3. Hysteretic loops without deterioration

Unloading from the envelope curve leads to another basic curve, e.g. the curve starting from the unloading point A in Fig. 3.1. In the figure, the point  $P_0(\varepsilon_{p0}, \sigma_{p0})$  and point  $N_0(\varepsilon_{n0}, \sigma_{n0})$

are the peak points in the positive and negative sides, respectively. A basic curve starts from the start point  $(\varepsilon_s, \sigma_s)$  that can be determined by the following equation, which is a modified version of Eqn. (3.6) by setting the original point to the start point  $(\varepsilon_s, \sigma_s)$ .

$$\sigma = \sigma_s + E(\varepsilon - \varepsilon_s) + (\varepsilon - \varepsilon_s)^2(3\sigma_m - 2E\varepsilon_m)/\varepsilon_m^2 + (\varepsilon - \varepsilon_s)^3(E\varepsilon_m - 2\sigma_m)/\varepsilon_m^3 \quad (3.8)$$

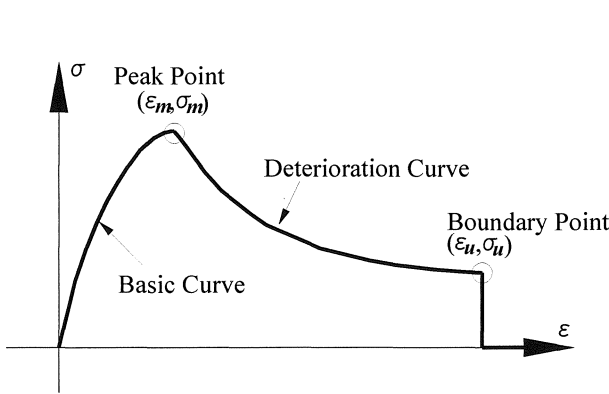


Figure 3.1. Envelope curves

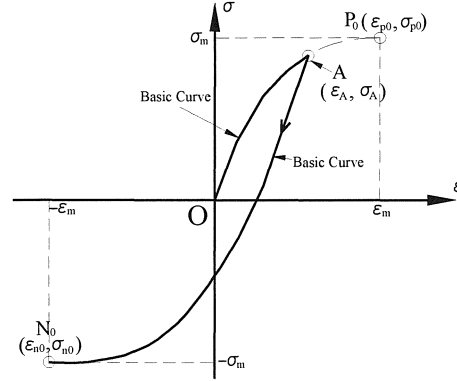


Figure 3.2. Cyclic basic curve

Therefore, new basic curves are generated by substituting the unloading point into the start point of Eqn. 3.8, in the case where the amplitude of the loops monotonically increase, as shown in Fig. 3.2 and the unloading stress  $\sigma_{un} = \sigma_B$  is larger than the starting stress  $\sigma_s = \sigma_A$  in the absolute value ( $|\sigma_{un}| > |\sigma_s|$ ). According to general observation of irregular hysteretic loops of steel structures, in the case where the amplitude decreases from former loops as shown in Fig. 3.3 and the stress of unloading point  $\sigma_{un} = \sigma_{B'}$ , is smaller than the starting stress  $\sigma_s = \sigma_A$  in absolute value ( $|\sigma_{un}| < |\sigma_s|$ ), the hysteretic loop usually shows a larger slope than the basic curve. This hardening effect, mentioned as unloading-reloading effect in the studies of reinforcement bars of RC structures, can be refined by introducing a curve (sub curve) obtained by omitting the cubic term of the basic curve, as in the following expression.

$$\sigma = \sigma_s + E(\varepsilon - \varepsilon_s) + (\varepsilon - \varepsilon_s)^2(\sigma_t - \sigma_s)/(\varepsilon_t - \varepsilon_s)^2 - E/(\varepsilon_t - \varepsilon_s) \quad (3.8)$$

where  $(\varepsilon_s, \sigma_s)$  represents the start point of the new sub curve as point B' ( $\varepsilon_{B'}, \sigma_{B'}$ ) for the sub curve B'A in Fig. 3.3, and  $(\varepsilon_t, \sigma_t)$  represents the target point of the new sub curve, which is the start point of the former curve or the last unloading point, as the point  $(\varepsilon_A, \sigma_A)$  in the figure.

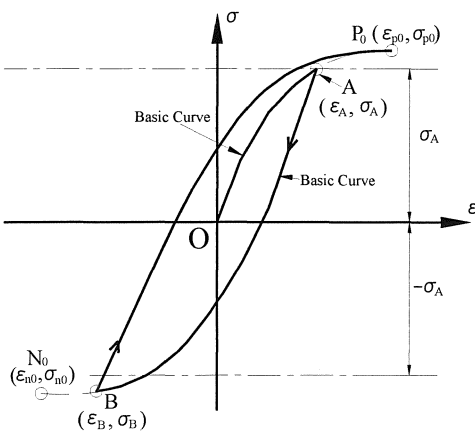


Figure 3.3. New basic curves increasing with amplitude

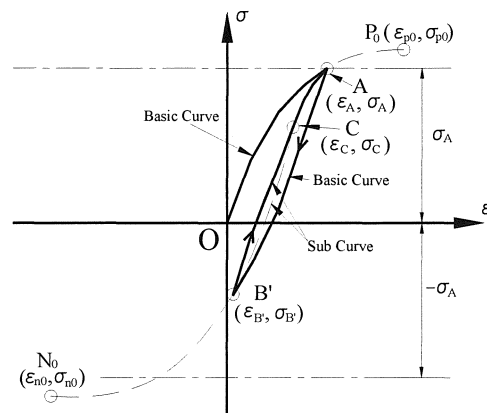


Figure 3.4. New sub curves with decreasing amplitude

### 3.4. Cumulative deterioration strain

The strain increment  $\Delta\varepsilon_{di}$  experienced in each loading step in the deterioration curve after the peak

strength resulted in not only the immediate decrease of bearing strength but also degeneration and softening of hysteretic loops after the unloading from the previous deterioration loop. These deterioration behaviours of steel piers, including (a) softening of the elastic modulus mentioned in section 3.5, (b) degeneration of peak points and (c) expansion of the distance between the peak points, can be recognized as the result of cumulative the damage of deterioration due to the out-of-plane deformation in constituent plates. The cumulative value of the deterioration strain increment, which is termed as the cumulative deterioration strain  $\varepsilon_{cd} = \sum |\Delta \varepsilon_{di}|$ , can be considered as a direct index to evaluate these effects.

### 3.5. Degeneration and softening of hysteretic loops

After deterioration, the elastic modulus  $E$  is usually reduced from the initial value  $E_0$  due to the residual out-of-plane deformation of web and flange plates. The following equation is introduced to approximate this softening phenomenon.

$$E = E_0 \left( 1 - \mu \frac{\varepsilon_{cd}}{\varepsilon_u - \varepsilon_{m0}} \right) \quad (3.9)$$

where the parameter  $\mu$ , which is smaller than unity and generally larger than 0.5 for stiffened columns, represents the softening ratio of the elastic modulus  $E$  after the cumulative deterioration strain increases to the deterioration ultimate boundary  $\varepsilon_u - \varepsilon_{m0}$ , and  $\varepsilon_{m0}$  is the initial peak point strain presented as  $\varepsilon_m$  in the envelope curve as in Fig. 3.1.

The peak points in both positive and negative loading directions in the hysteretic loops after deteriorating are usually degenerated to a lower strength, but their strain distance (related position) gradually increases. The new peak point in the loading direction side towards to the point of the most recent deterioration, the positive-side peak load point in Fig. 3.5 as an example, can be considered as the unloading point from the deterioration curve,  $P_i(\varepsilon_{pi}, \sigma_{pi})$  in the figure. And the peak point on the opposite side, point  $N_i(\varepsilon_{ni}, \sigma_{ni})$  in the figure, is set by sharing the same stress deterioration with the deteriorated side ( $\sigma_{ni} = -\sigma_{pi}$ ) and shifting its strain position with a strain distance denoted by  $D_m$  from the original position  $N_0(\varepsilon_{n0}, \sigma_{n0})$ . The distance between two peak points  $D_m$  is initially equal to  $D_{m0} = 2\varepsilon_{m0}$ , and usually increases with the cumulative value of deterioration as in the following equation.

$$D_m = D_{m0} \left( 1 + \gamma \frac{\varepsilon_{cd}}{\varepsilon_u - \varepsilon_{m0}} \right) \quad (3.10)$$

The parameter  $\gamma$ , which is zero for thick-walled steel columns and generally less than unit, represents the degree of degeneration and softening of the hysteretic loops.

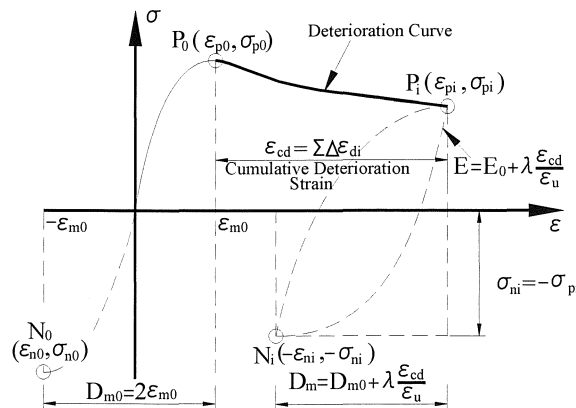


Figure 3.5. Upgrade peak points post deterioration

## 4. PSEUDODYNAMIC TESTS AND VALIDATION

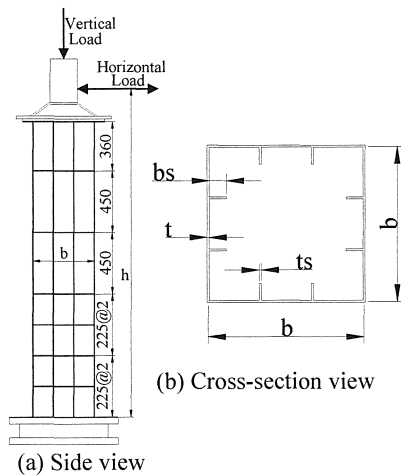


Figure 4.1. Test specimen dimensions

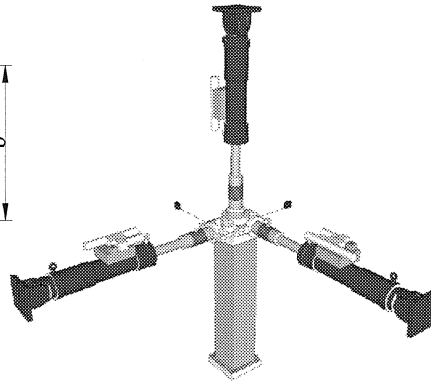


Figure 4.2. Loading system

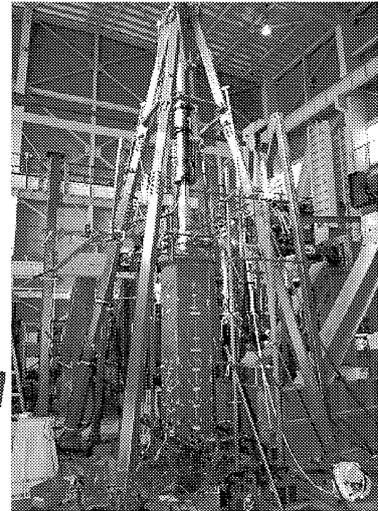


Figure 4.3. Test set-up

### 4.1. Tests description

The side view and cross-sectional view of the test specimens are shown in Fig. 4.1. All the test pier specimens were fabricated with stiffened square 450 mm  $\times$  450 mm cross-section of plate thickness 6 mm. Two vertical stiffeners of 55 mm width is used on each web or flange plate, and diaphragms are placed with 225 mm interval distance. The plates were made of SM490 grade steel, whose nominal yield strength is 325 N/mm<sup>2</sup>. The width-to-thickness parameters  $R_R$  and  $R_F$  are 0.517 and 0.178, respectively. The slenderness parameter  $\lambda$  is 0.344 and the slenderness parameter of stiffener  $\lambda_s$  is 0.184.

Three actuators (1000 kN capacity) were set in the two orthogonal horizontal directions and vertical direction, as shown in Fig. 4.2. Applying the loads by operating these actuators, three-dimensional loading tests for cantilever type bridge columns can be conducted as shown in Fig 4.3. Uni- and bi-directional loading the pseudodynamic tests under constant vertical loads were conducted by this loading system, and preliminary quasi-static loading tests were also conducted using a specimen of the same type to identify the hysteretic parameters for the MS model implementing the constitutive laws with approximated curves described in the Chapter 3.

Three sets of ground motions including the two orthogonal horizontal components (NS and EW) of, namely JMA Kobe, Takatori, and Port Island records during the 1995 Kobe Earthquake were used as the input accelerograms in the pseudodynamic tests. Accordingly, six uni-directional loading tests and three bi-directional loading pseudodynamic tests were performed. The test programme including the input earthquakes are listed in Table.4.1.

### 4.2. Comparison of test and simulation results

Uni- and bi-directional loading seismic response simulation applying the MS model with the hysteretic constitutive laws using the approximated curves were also conducted, by applying the structure models and ground motions identical to that of the pseudodynamic tests. Maximum values of the horizontal force and response displacement in the NS and EW directions of the piers obtained by separate or simultaneous loading tests or simulation are listed in Table.4.1. In this table, value of the maximum horizontal force and the maximum response due to the bi-directional loading tests or simulation are given not only in NS, EW directions but also those in oblique directions, as marked in the "Directions" column. The maximum force or the maximum response displacement in oblique directions is the maximum value of the resultant force or superposition of the responses. Values with brackets in cells for the maximum displacement of test PKB-2D are the maximum values until the test

was stopped due to excessive large deformation and serious damage in the constituent plates. Moreover, hysteretic restoring force-displacement relationships under by bi-directional loading obtained by the tests and simulations are plotted in Fig. 4.4 with solid (tests) and broken lines (simulation), respectively.

**Table 4.1.** List of the test cases

Name	Earthquake (Ground Type)	Loading method	Directions	Maximum Horizontal Force ( $H_{max}/H_0$ )			Maximum response displacement ( $\delta_{max}/\delta_0$ )		
				Test	Sim	Error(%)	Test	Sim	Error(%)
JMA-NS	Japan Metro Association (I)	Uni-directional	NS	1.56	1.69	8.38	3.68	3.66	0.65
JMA-EW			EW	1.86	1.69	9.30	2.86	2.90	1.23
JMA-2D		Bi-directional	NS	1.42	1.44	1.80	2.82	2.87	1.61
			EW	1.31	1.51	14.7	2.31	2.36	2.18
	Oblique		1.49	1.52	1.57	3.33	3.36	0.86	
JRT-NS	Japan Railway Takatori (II)	Uni-directional	NS	1.81	1.69	6.30	5.46	5.37	1.55
JRT-EW			EW	1.66	1.69	1.77	4.82	4.22	12.6
JRT-2D		Bi-directional	NS	1.50	1.41	6.06	6.59	7.48	13.5
			EW	1.65	1.54	6.56	4.04	4.17	3.44
	Oblique		1.71	1.62	4.89	7.40	8.22	11.1	
PKB-NS	Port-island Kobe Bridge (III)	Uni-directional	NS	1.64	1.69	3.15	5.18	4.95	4.47
PKB-EW			EW	1.72	1.69	1.86	5.70	5.20	8.66
PKB-2D		Bi-directional	NS	1.45	1.41	2.23	(12.8)	10.0	—
			EW	1.11	1.31	18.4	(9.77)	8.50	—
	Oblique		1.55	1.58	2.17	(15.8)	12.8	—	

\*JMA= JMA Kobe, JRT= Takatori, PKB=Port Island

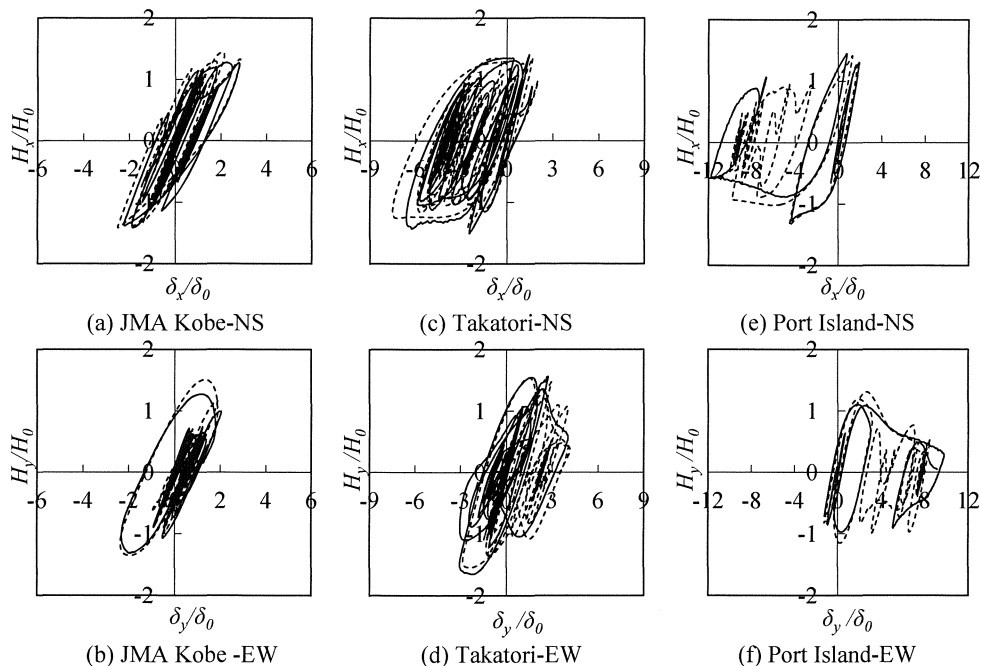


**Figure 4.4.** Hysteretic relationship obtained by tests (solid lines) and simulation (broken lines)

As shown in the figure, the hysteretic loops obtained by the bi-directional loading hybrid tests show sudden decrease and discontinuous softening due to the coupled inelastic effects in the two lateral directions, which have also been simulated by the MS model analysis using the proposed hysteretic laws. Comparison between the tests and simulations listed in the table also demonstrated that the maximum horizontal force by tests and simulation are generally in good agreement. Although the maximum difference (error) between the tests and simulations is reaches approximately 18%, the average error for all cases is as small as 6% including that of bearing capacity deflection caused by

specimen fabrication which is typically 5% as the average and 8% as the maximum value, as observed from the comparison of the uni-directional loading tests only.

The response displacements obtained by the loading tests and numerical simulations are also in agreement as shown in Fig. 4.4. Response and hysteretic behaviours of rectangular stiffened hollow steel columns under bi-directional earthquake excitation are captured by the simulation with high fidelity as can be seen in the figures, and the relative error is approximately 5% in average excluding the test PKB-2D, which was stopped due to large deformation and damage.

## 5. CONCLUDING REMARKS

This study presents a three-dimensional numerical analysis method for simulating nonlinear seismic response of thin-walled square-section steel columns under bi-directional horizontal excitation and constant vertical loads. Rectangular sections of hollow steel columns, which is generally stiffened by longitudinal stiffeners, are equivalently considered as a series of springs distributed along the section with 2-dimensional coordinates and tributary areas. The basic elastic stiffness of the spring can be identified from the formula for the relationship between displacement and strain and resulting horizontal force from integration of stress derived from the plan section assumption.

Inelastic hysteretic rules for the relationship between springs' stress and strain exploited the constitutive laws with the approximated curves of a hysteretic restoring force-displacement model for SDOF nonlinear analysis. The stress-strain constitutive model using the approximated curves employs cubic or quadratic curves as the basic curve, sub curve and deterioration curves to smoothly approximate the inelastic behaviours of thin-walled steel columns. Reduction of bearing capacity after the peak strength, degeneration and softening of hysteretic loops after deterioration are also considered in this stress-strain constitutive model.

Uni- and bi-directional horizontal loading pseudodynamic online test results demonstrated the validity and effectiveness of this numerical analysis method. The difference between tests and simulation are adequately small, resulted in the relative error of the peak horizontal force of approximately 6% and that of maximum response of 5% in average.

## REFERENCES

- Aoki, T., Ohnishi A., Suzuki M. (2007). Experimental Study on the Seismic Resistance Performance of Steel Bridge Piers Subjected to Bi-Directional Horizontal Loads. *Journal of Japan Society of Civil Engineers*. **64:4**, 716-726.
- Dang, J., Nakamura, T., Aoki, T., Suzuki, M. (2010). Bi-Direcitional Loading Hybrid Test of Square Section Steel Piers. *Journal of Structure Engineering(JSCE)*. **56:A**, 367-380.
- Dang, J., Aoki, T.(2010). The Cubic Curves Hysteresis Model of Steel Bridge Piers for Seismic Response Simulation, *Pacific Structure Steel Conference, Beijing*, **Vol 9**: 1202-1216.
- Editorial Committee of the Report for Investigation of the Great Hanshin-Awaji Earthquake. (2002). the Report for Investigation of the Great Hanshin-Awaji Earthquake, Maruzen
- Goto, Y., Jiang K., Obata M. (2005). Hysteretic Behavior Of Thin-Walled Circular Steel Columns under Cyclic Bi-Axial Loading. *Journal of Japan Society of Civil Engineers*. **780:1-70**, 181-198.
- Goto, Y., Jiang K., Obata M. (2007). Hysteretic Behavior of Thin-Walled Stiffened Rectangular Steel Columns under Cyclic Bi-Directional Loading. *Journal of Japan Society of Civil Engineers*. **63:1**, 122-141.
- Goto, Y., Koyama R., Fujii, Y., Obata M. (2009). Ultimate State of Thin-Walled Stiffened Retangular Steel Columns under Bi-Directional Seismic Excitations. *Journal of Japan Society of Civil Engineers*. **65:1**, 61-80.
- Ishii, K., Kikuchi, M., Kato, H. (2010). A New Analytical Model for Elastomeric Seismic Isolation Bearings under Multiaxial Loading, *Proceeding of Japan Earthquake Engineering Symposium*. **Vol 13**: 480-485.
- Ishizawa, T., Iura, M. (2006). One-Dimensional Analysis of Box Section Steel Bridge Piers, *Journal of Japan Society of Civil Engineers*. **62:2**, 288-299.
- Japan Road Association. (2002). Specifications for Highway Bridges. Maruzen

- Jiang, L., Goto, Y., Obata, M.(2001). Multiple Spring Model for 3D-Hysteretic Behavior of Thin-Walled Circular Steel Piers, *Journal of Japan Society of Civil Engineers*. **689:1-57**, 1-17.
- Jiang, L., Goto, Y., Obata, M.(2002): Hysteretic modeling of thin-walled circular steel columns under biaxial bending, *Journal of Structure Engineering (ASCE)*, **128:3**, 319-327.
- Kuroda, E. (2001), Engineering Calculation Program Based on Visual Basic, CQ
- Lai, S., Will, G. T., Otani, S. (1984). Model for Inelastic Biaxial Bending of Concrete Members, *Journal of Structure Engineering (ASCE)*, **110:11**, 2563-2584.
- Nagata, K., Watanabe, E., Sugiura, K. (2004). Elasto-plastic Response of Box Steel Piers Subjected to Strong Ground Motion in Horizontal 2 Directional. *Journal of Structure Engineering(JSCE)*. **50:A**, 1427-1436.
- Sakimoto, T., Watanabe, H., Nakashima, K. (2000). Hysteetic Models of Steel Box Members with Local Buckling Damage. *Journal of Japan Society of Civil Engineers*. **647:1-51**, 343-355.
- Usami, T., Japan Society of Steel Structure. (2006), Guidelines for Seismic and Damage Control Design of Steel Bridges, Gihodoshuppan
- Watanabe, E., Sugiura, K. and Oyawa, W.O.(2005) Effects of Multi-Directional Displacement Paths on the Cyclic Behaviour of Rectangular Hollow Steel Columns. *Journal of Japan Society of Civil Engineers*. **647:1-51**, 29-48.